Exoskeleton Energetics: Implications for Planetary Extravehicular Activity

Christopher E. Carr
Massachusetts Institute of Technology
77 Massachusetts Ave
Room 54-418
Cambridge, MA 02139
617-253-0786
chrisc@mit.edu

Dava J. Newman
Massachusetts Institute of Technology
77 Massachusetts Ave
Room 33-307
Cambridge, MA 02139
617-258-8799
dnewman@mit.edu

***Abstract*—Humans first visited another world nearly 50 years ago and are poised to return to the Moon and visit Mars in the coming decade(s). Developing a space suit that supports safe, efficient, and effective exploration despite the extremes of temperature, pressure, radiation, and environmental hazards like dust and topography remains a critical challenge. Space suits impose restrictions on movement that increase metabolic rate and limit the intensity and duration of extravehicular activity. In this study, a lower body exoskeleton was used to test a simple model that predicts the energy cost of locomotion across gait and gravity. Energetic cost and other variables were measured during treadmill locomotion, with and without a lower body exoskeleton, in simulated reduced gravity and in Earth gravity. Six subjects walked and ran at constant Froude numbers, non-dimensional parameters used to characterize gait. The spring-like energy recovery of the exoskeleton legs was estimated using energetics data in combination with the model. Model predictions agreed with the observed results (no statistical difference). High spring-like energy recovery of the exoskeleton legs lowered measures of the energetic cost of locomotion. For planetary extravehicular activity, our work reveals potential approaches to optimizing space suits for efficient locomotion, for example, tuning the stiffness and spring-like energy recovery of space suit legs.**

TABLE OF CONTENTS

1. INTRODUCTION

NASA's long term Mars exploration goals include humans exploring the surface of that planet [1]. SpaceX has painted an expansive vision for human exploration of Mars [2]. Future visitors or inhabitants there are not going with the intention to stay safely inside their habitats, but to explore–and build–a new world: for example, to search for life beyond Earth [3], and to find the resources required for continued human habitation [4].

Space suits adversely impact the achievable mechanical efficiency of work, limit mobility, and increase the metabolic costs of locomotion relative to unsuited conditions [5]. Prior regression modeling of historical unsuited and suited energetics data suggested that space suits may act as springs during running [6].

We previously characterized a lower-body exoskeleton that induces joint-torques similar in form and magnitude [7] to the knees of the extravehicular mobility unit (EMU), NASA's current space suit for orbital operations. The legs of this exoskeleton function as non-linear springs, similar to how space suit legs function during running. However, locomotion performance in the exoskeleton is likely to differ from performance in otherwise similar conditions in a space suit because of the substantial differences between the two. While space suits significantly impair hip mobility [8], the exoskeleton has generally good hip mobility [7]. These differences are beneficial, because they permit the isolation and study of different contributions to the effect of space suits on locomotion energetics.

Objectives

Here we:

(1) Test a simple model of locomotion energetics that predicts the energy cost of locomotion across gait and gravity;

(2) Use this model to characterize how a lower-body exoskeleton modifies the energetics of walking and running; and

(3) Apply our findings to understand the implications for space suits in the context of planetary extravehicular activity (EVA).

Overview

We first develop the locomotion energetics model and describe our experimental procedures in Section 2. Next, we describe experimental results, model validation, and the energetic impacts of exoskeleton locomotion in Section 3. We then explore the caveats and implications of our results in Section 4. Finally, we summarize our contributions in Section 5. Mathematical derivations underlying our modeling of human muscle efficiency are found in the appendices, and additional details can be found in [9].

978-1-5090-1613-6/17/31.00

2. METHODS

Model Development

We have previously shown [5] that the net metabolic rate, $\dot{Q}_{loco}$ [W], during locomotion can be represented as

$$\dot{Q}_{loco} = \dot{Q}_m - \dot{Q}_B = \frac{\dot{W}(1-\eta)}{E}, \quad (1)$$

with total metabolic rate $\dot{Q}_m$, basal metabolic rate $\dot{Q}_B$, total rate of forward and vertical work done on the center of mass $\dot{W}$ [W], and the two non-dimensional quantities energy recovery η, and muscle efficiency E. We briefly describe each parameter.

The metabolic rate $\dot{Q}_m$ represents the total rate of enthalpy change during locomotion, whereas $\dot{Q}_B$ represents the rate of enthalpy change required during rest. Thus $\dot{Q}_{loco}$ is the change in enthalpy associated with locomotion. $\dot{Q}_m$ and $\dot{Q}_B$ can be measured on a breath-to-breath basis by simultaneously monitoring oxygen consumption and carbon dioxide production, during locomotion and at rest, respectively. $\dot{W}$ can be measured from kinematic analysis to estimate center of mass movements. As is customary, we normalize $\dot{Q}_m$ by mass m to give mass-specific metabolic rate $\dot{Q}_{m,kg}$ $[W/kg]$, and further normalize by velocity to give mass-specific cost of transport $C_m = \dot{Q}_{m,kg}/v$ $[J/(m \cdot kg)]$. Finally, we normalize by gravitational acceleration to give specific resistance $S = C_m/g$ $[J/(N \cdot m)]$. This non-dimensional parameter represents the amount of energy required to transport a load of unit weight a unit distance.

Energy recovery η quantifies the reversibility of work being done on the center of mass. For example, imagine a mass on a perfect spring (no damping) oscillating up and down; once set in motion, this mass would oscillate forever, because any work done on the spring, e.g., through converting gravitational potential to spring compression, would be recovered through spring extension. This corresponds to $\eta = 1$. In contrast, compressing a "spring" that has no rebound force corresponds to $\eta = 0$. Griffin et al. [10] report data for η for walking as a function of velocity and G-level. Using data from Kaneko [11], we previously derived that $\eta = 0.55$ for human running near the run-walk transition, and declines at high speeds [5].

Muscle efficiency E is defined as the rate of mechanical work to enthalpy change, or equivalently, the mechanical power produced by a fully activated muscle compared to the metabolic power consumption. In classic studies of muscular efficiency, Margaria [12] estimated peak $E = 0.25$, although the modern validated Hill muscle model, which reflects the molecular basis of muscle activation and has been validated across multiple vertebrate species, gives peak $E = 0.23$ (derivation in Appendix A).

We assume human muscles operate near peak efficiency, a reasonable assumption given that similar (within $2-3\%$) estimates for efficiency have been obtained for walking [12] or cycling [13].

Hypotheses

We hypothesized that our model (Equation 1) would be able to explain changes in locomotion energetics across G-levels and across gait {walking, running}. We further hypothesized that the addition of exoskeleton legs, which act as high energy recovery springs, would elevate the energy recovery in both walking and running. As a result, we expected this to reduce the cost of transport $[J/(kg \cdot m)]$ and specific resistance $[J/(N \cdot m)]$ relative to the unsuited condition in reduced gravity conditions, whereas in Earth-gravity conditions we expected the increase in recovery might come at the expense of total metabolic rate, just as it does in space suits. We now describe the experimental protocol used to test these hypotheses.

Experimental Protocol

Six subjects, three men and three women, participated in the experiment after giving informed consent. Each subject attended an introductory session involving anthropometric measurements, fitting of an exoskeleton (Figure 1A-B, [7]), and an exoskeleton familiarization period. Subjects completed the primary session on a separate day.

For the primary session, all subjects completed the same sequence of three trials over a several hour period in a single day (Figure 1C). Subjects ran and walked during the first trial in an *unsuited* condition, wearing normal athletic shoes. In the second trial, denoted as the *ExoControl* condition, subjects wore the lower-body exoskeleton with fiberglass bars (springs) of intermediate thickness (0.3175 cm or 0.125 in). In the *ExoControl* condition, the intermediate thickness springs were used with the intention to simulate the restrictions of motion of the exoskeleton without the effect of stiff legs. In the third trial, denoted as the *Exoskeleton* condition, subjects wore the lower-body exoskeleton with springs of thickness 0.635 cm (0.250 in), intended to simulate the knee torques of the EMU.

Trials included ten three-minute stages: an initial basal metabolic measurement stage, and three gravity conditions (G_{Moon}, G_{Mars}, G_{Earth}) each with three stages. For the first and last stages during each gravity condition, subjects walked or ran for the entire three-minute stage at a specified Froude number, a non-dimensional velocity given by

$$Fr = \frac{v^2}{gL}, \quad (2)$$

where Fr is the Froude number, v is the treadmill velocity, L is the leg length, and g is the simulated gravity level given by $g = g_{earth} \cdot G$, with Earth relative gravity G and Earth gravity taken as $g_{earth} = 9.81 m/s^2$ ($G_{earth} = 1$). Froude numbers prescribed for walking and running conditions were 0.25 and 0.60, respectively.

In the middle stage during each gravity condition, subjects walked or ran at a self-selected run-walk transition, also called the preferred transition speed (PTS). To select this speed, subjects switched gaits several times in a consistent controlled fashion (Figure 1C).

Moon and Mars conditions were simulated using the Moonwalker, a spring-based partial body-weight suspension system (Figure 1D) [9]. The {Moon, Mars, Earth} order of simulated gravity levels was intended to increase workload

over time (limit fatigue), provide experience before operating the exoskeleton at $G = 1$ (safety), and improve subject comfort over time [9].

While the G-level was adjusted, the subject stood flat-footed on the treadmill, occasionally making small hops at the indication of the experiment conductor who monitoring the real-time G-level. These hops helped to eliminate the effects of stiction on the observed G-level, which was estimated for display as,

$$G = 1 - \frac{F}{m_{total} \cdot g_{earth}}, \tag{3}$$

where F is the net upward force on the total transported mass m_{total}. The total transported mass m_{total} was determined by weighing the subject along with shoes, harness, and if applicable, the exoskeleton, using the Moonwalker load cell during the first gravity adjustment session in each trial. All masses except body mass were already known, and body mass was computed as the difference between total mass and known masses.

Treadmill (Trotter CXT^{Plus}, Cybex Corporation, Medway, MA) velocities for each prescribed Froude number stage were calculated in real-time based on the actual G-level (obtained during G-level adjustment) and the subject leg length (measured during a prior introductory session). The test conductor adjusted the velocity of the treadmill, and the treadmill velocity display was obscured from the subject's view.

Data Collection

A metabolic analyzer (VO2000, MedGraphics, St. Paul, Minnesota), auto-calibrated on room air before each trial, recorded O_2 consumption and CO_2 production rates throughout each trial by sampling expired air from a special facemask system with flow-sensing capability. Data from the last minute of each stage was analyzed based on prior validation of this time period as approximating quasi-steady-state conditions. Subjects wore a heart rate monitor, and an accelerometer (CXL10LP3, Crossbow Technology, San Jose, California) mounted near the center of mass (lower back).

Analog signals from the treadmill (rotations of the rear roller as a measure of velocity), moonwalker load cell, and gait accelerometer were simultaneously sampled and digitized at 1 kHz (PMD-1608FS, Measurement Computing, Middleboro, MA) and logged via custom scripts implemented in MATLAB (The Mathworks, Natick, Massachusetts).

Gait Analysis

Due to the lack of kinematic (motion tracking) or kinetic (force plate) measurements; gait analysis consisted of computing the Froude number and cadence for each sub-stage condition.

The actual Froude number achieved in each condition was computed using the measured treadmill velocity, the subject leg length, and the actual mean G-level achieved over the sub-stage condition.

Cadence (step frequency), denoted by f, was calculated using a combination of accelerometer and moonwalker load-cell data depending upon which had better quality [9].

Non-dimensional cadence was computed as

$$\Lambda = \frac{fL}{v}, \tag{4}$$

where Λ is the non-dimensional cadence, L is subject leg length and v is the treadmill velocity. If ψ is the excursion angle swept out by the leg during a single stance period (Appendix C), then the non-dimensional cadence is related to the excursion angle during an idealized compass gait (with no double support and no aerial phase) by

$$\Lambda = \frac{1}{2sin\left(\frac{\psi}{2}\right)}. \tag{5}$$

Because actual gait normally involves either a double support phase (in walking) or an aerial phase (in running[1]), Equation 5 can be adjusted to read

$$\begin{array}{ll} \Lambda \geq \frac{1}{2sin\left(\frac{\psi}{2}\right)} & \text{for walking, or} \\ \Lambda \leq \frac{1}{2sin\left(\frac{\psi}{2}\right)} & \text{for running.} \end{array} \tag{6}$$

If one compared Λ values for walking and running, one would expect the observed differences to originate from differences in the excursion angle or the magnitudes of the double support phase (in walking) or aerial phase (in running). Non-divergence would imply either similar excursion angles, or a change in the excursion angle that counteracts the effects of the double support and/or aerial phase.

Energetic Analysis

Metabolic rate $\dot{Q}_m$ [W] was estimated by multiplying the O_2 consumption rate by the conversion factor, $k\ [W]/[mlO_2/s]$,

$$k = 4.33 \cdot RQ + 16.6, \tag{7}$$

where RQ is the respiration quotient, the ratio of moles of oxygen consumed to carbon dioxide expelled. The constants in Equation 7 are standard values for the free energy released from metabolism of oxygen and food at the specified respiration quotient. Mass-specific metabolic rate $\dot{Q}_{m,kg}$, mass-specific cost of transport $C_m = \dot{Q}_{m,kg}/v$, and specific resistance $S = C_m/g$ were estimated using the total mass transported, m_{total}.

To test the model of locomotion energetics across gravity levels, specific resistance for {reduced gravity, unsuited} conditions was estimated based on the {Earth gravity, unsuited} condition.

First, we computed the net cost of locomotion, $\dot{Q}_{loco} = \dot{Q}_m - \dot{Q}_b$. Recovery, η was estimated as a function of v and G using data from [10] for walking, or taken as $\eta = 0.55$ for running, while muscle efficiency, E_{musc} was estimated as a function of G using the Hill model (see Appendix B for details on the gravitational dependence of E_{musc}).

[1] Groucho running [15] excepted.

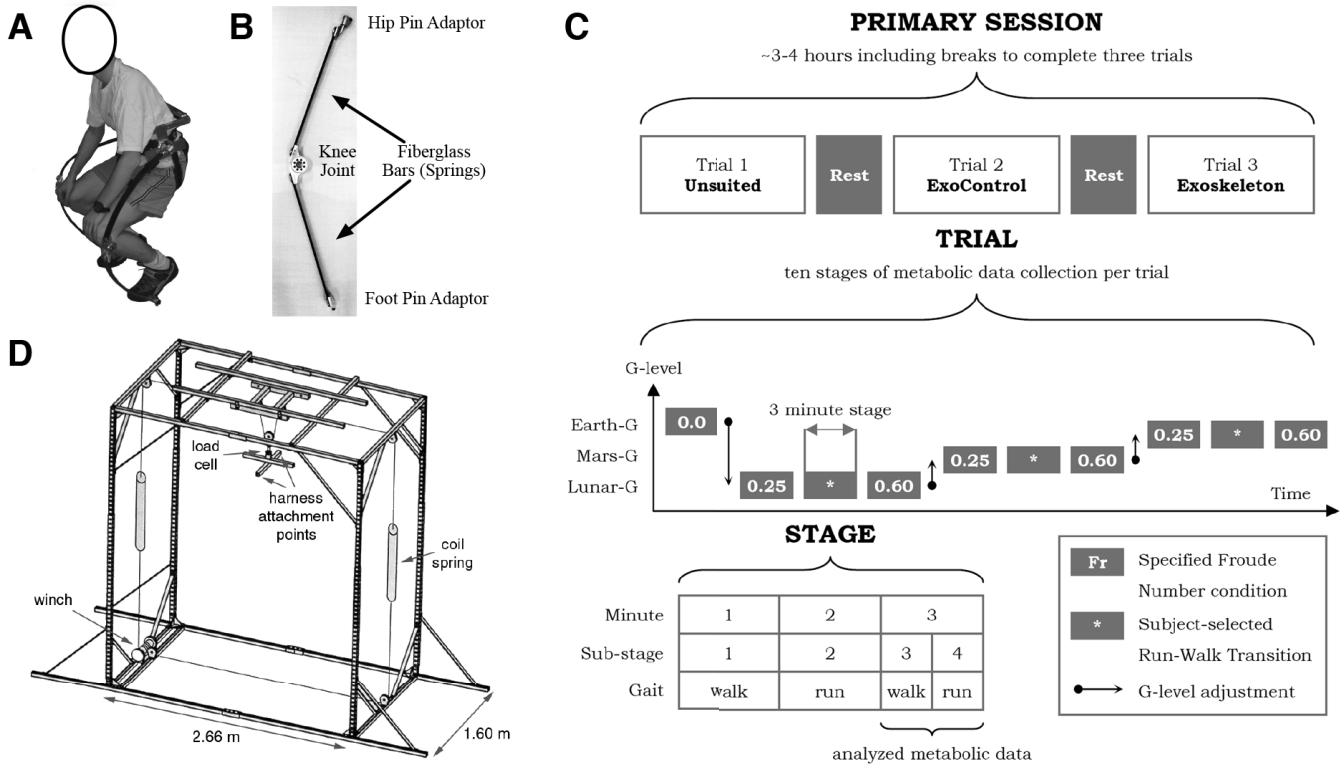

Figure 1. Experiment Apparatus and Design. A) Lower body exoskeleton. The exoskeleton is donned via a waist harness and adjustable hip cage. Exoskeleton legs are connected between a 2 degree of freedom (DOF) hip joint and a one DOF joint on the lateral forefoot of a modified cycling shoe [7]. B) Each exoskeleton leg is made of two fiberglass bars connected via knee joint. Different length bars and knee angles can be selected to accommodate a range of subject sizes and approximate the joint torques of the EMU knee joints. These selections were made during the exoskeleton familiarization period. C) Experiment Design (see text for details). D) The Moonwalker [14] is a partial body-weight suspension device with three DOF: front-rear translation, vertical translation, and yaw rotation. Subjects used a centrally-located treadmill. Suspension was via a winch driven cable that controlled the displacement of coil springs connected via a load cell to the subject's harness.

The total positive work rate of the locomotion muscles was then estimated as

$$\dot{W}_{in} = \dot{Q}_{loco} \cdot \frac{E_{musc}}{1-\eta}. \tag{8}$$

where $\dot{W}_{in}$ is the total positive work rate of the locomotion muscles. The total rate of positive work done on the center of mass in a different condition (indicated with a prime, $'$), assuming similar kinematics and kinetics that scale directly with mass and gravity, can be estimated as

$$\dot{W}'_{in} = \dot{W}_{in} \cdot \frac{G'}{G} \cdot \frac{m'}{m}. \tag{9}$$

From this result, Equation 8 can be used to solve for the new net cost of locomotion,

$$\dot{Q}'_{loco} = \dot{W}'_{in} \cdot \frac{1-\eta'}{E'_{musc}}, \tag{10}$$

which gives

$$\dot{Q}'_{m} = \dot{Q}'_{loco} + \dot{Q}_{b}, \tag{11}$$

and finally

$$S' = \frac{\dot{Q}'_{m}}{m' \cdot g' \cdot v'}. \tag{12}$$

In order to estimate the impact of the ExoControl and Exoskeleton conditions on recovery, we performed a related procedure. First, $\dot{W}_{in}$ was estimated from the measured metabolic data at each G-level in the unsuited condition. $\dot{W}'_{in}$ was then calculated for each corresponding ExoControl or Exoskeleton condition. This $\dot{W}'_{in}$ value, taken together with the measured S in each condition, was used to estimate the net energy recovery of the hybrid human-exoskeleton system according to

$$\eta' = 1 - \frac{\dot{Q}'_{loco} \cdot E'_{musc}}{\dot{W}'_{in}}. \tag{13}$$

3. RESULTS

Subject, exoskeleton, and experiment characteristics are given in Table 1. Individual subject characteristics, exoskeleton customization data, and other individual results and details are reported in [9]. Except as otherwise described, p-values are two-sided and based on regression with effects coding of categories, treating subjects as a random intercept.

The mean EMU-relative stiffness for the exoskeletons used by the subjects was unity, implying that on average the exoskeletons were excellent matches for EMU knee joints.

While basal metabolism measurements were highly variable, the mean mass-specific basal metabolic rates observed under the ExoControl and Exoskeleton conditions were not significantly different than the unsuited condition. The overall mass-specific basal metabolism was $\dot{Q}_{b,kg}$ was 1.51 ± 0.15 [W/kg] across all conditions and subjects.

In general, slightly lower G-levels were achieved than desired, averaging 5% below the target. In contrast, actual walking speed (Fr) errors increased at lower G-levels. At Mars and Lunar G-levels, the 0.045 (0.1 mph) resolution of the Treadmill velocity can generate errors as high as 5.0% and 7.6% respectively in the target Fr (Lunar RMS error is expected to be 4.5%). Thus, one component of the errors observed for {Mars, Walking} and {Moon, Running} conditions is due to the limited treadmill velocity resolution.

Exolocomotion Gait

Cadence values, shown in Figure 2A, decline with reductions in gravity ($p < 0.0005$), and have a significant spread between the walking and running cadence values ($p < 0.0005$). Non-dimensional cadence values, shown in Figure 2B, still have a significant spread between the walking and running cadence values ($p < 0.0005$), but the spread is opposite in sign and half the magnitude of the dimensional cadence spread, with Λ values for running lower than Λ values for walking. Unlike f, the Λ values increase with reductions in gravity ($p < 0.0005$).

Self-selected run-walk Froude numbers increased as $G-$level decreased ($p < 0.0005$), reaching a median value of 0.81 in the Lunar condition (Figure 2C). Median and mean self-selected run-walk Froude numbers were lower for the ExoControl and Exoskeleton conditions ($p < 0.0005$) as compared to the Unsuited condition.

Exolocomotion Energetics

Mass-specific metabolic cost [W/kg], shown in Figure 3 (top), increased with G-level and Froude number, and was significantly lower for ExoControl and Exoskeleton conditions in comparison to the Unsuited condition (all $p < 0.0005$). However, the highest absolute mass-specific metabolic cost occurred in the {Exoskeleton, running, Earth gravity} condition, which also had the highest mean metabolic cost.

During unsuited walking, cost of transport [$J/(kg \cdot m)$] was found to increase with reductions in gravity (Figure 3, center, $p = 0.001$). In the running and run/walk unsuited conditions, changes in gravity did not lead to a significant change in the cost of transport. In the ExoControl and Exoskeleton walking conditions, changes in gravity also did not lead to significant changes in cost of transport. However, during the run/walk and running conditions, cost of transport declined as gravity was reduced for both ExoControl and Exoskeleton conditions ($p \leq 0.014$).

Specific resistance [$J/(N \cdot m)$] (Figure 3, bottom) significantly increased with G-level reduction across all three exoskeleton conditions (Unsuited, ExoControl, Excoskeleton; $p < 0.0005$). Specific resistance was, on average, higher in the unsuited condition and lower in the ExoControl and Exoskeleton conditions. There was also a negative association with increases in the Froude number ($p = 0.023$), and a significant cross effect with the exoskeleton configuration and the G-level (Figure 3B).

Evaluating the Model

The measured and theoretical S values for the Unsuited condition, shown in Figure 4A, are in excellent agreement. In the walking ($Fr = 0.25$) condition, the theoretical estimates differ from the measured estimates by -17% and 4.5% for Lunar and Mars conditions, respectively. In the running ($Fr = 0.60$) condition, the estimates differ by only 8.7% and 3.4%. These error are comparable in size to the errors in controlling the Froude number or the errors in setting the G-level. None of these differences were significant (Table 2).

Impact of Exoskeleton on Energy Recovery

Unsuited values for energy recovery, shown in Figure 4B, represent input values based on the literature [10], [11], used to estimate the positive work done on the center of mass in each G-level condition. Presence of the exoskeleton, either in the ExoControl or Exoskeleton conditions, elevated the computed net energy recovery substantially, and more than counteracted the decline in energy recovery associated with unsuited walking as gravity is reduced. Walking recovery was elevated more than running recovery in Earth- and Mars-gravity conditions.

4. DISCUSSION

General Considerations

Our repeated measures experiment design prevented order effects from being analyzed, yet was a reasonable compromise to limit subject fatigue and achieve a low subject drop-out rate; despite a few cases where subjects were not able to maintain 1-g running, no subjects dropped out.

Basal metabolic rate measurements were variable, in part due to low flow with use of a high-flow pneumotach required for subsequent measurements. However, the basal metabolic rate averaged across all trials and subjects (1.51 ± 0.15 (SE)) compares favorably with [16], who found basal metabolic rate to be independent of gravity and equal to 1.47 ± 0.112 (SE) W/kg ($N = 4$).

Specified Froude numbers were significantly different from their target values; the non-constant force nature of the moonwalker springs made the moonwalker applied load vary significantly with body position, directly contributing to the larger Froude numbers errors at greater reductions in gravity. In $G = 1$ conditions, the Froude number errors are largely explained by the quantization error of the indicated treadmill velocity. While greater uniformity in setting G-levels and locomotion velocities (Fr) would be desirable for comparing between conditions, it does not impact our interpretation of the model because that utilized actual G-levels achieved, not imposed categories.

Table 1. **Subject and Experiment Characteristics**

Parameter	Mean	Std. Dev.	N[a]	Std. Err.	Notes
Subjects					
Age [years]	23.1	2.5	5	1.1	Excluding one 40 year old subject
Height [cm]	171	5.6	6	2.3	
Leg Length [cm]	88.6	3.4	6	1.4	
Ratio	1.93	0.09	6	0.04	Height / Leg Length
Body Mass [kg]	64.60	5.60	6	2.29	Light athletic clothing, no shoes
Exoskeleton					
Spring Length [cm]	43.2		5		One subject used 49.5 cm springs
Forward offset [cm]	12.7	1.4	6	0.6	See [7] Figure 3
Vertical offset [cm]	7.58	1.39	6	0.57	See [7] Figure 3
Knee angle [°]	40.0	1.7	6	0.7	See [7] Figure 3
Stiffness	1.00	0.10	6	0.04	Relative to EMU
Mass, ExoControl [kg]	6.78	0.14	6	0.06	Variation: spring length, shoe size
Mass, Exoskeleton [kg]	7.13	0.14	6	0.06	Variation: spring length, shoe size
Total Transported Mass [kg]					
Unsuited	66.20	5.70	6	2.33	Including shoes
ExoControl	72.30	5.70	6	2.33	Subject and Exoskeleton
ExoSkeleton	72.70	5.80	6	2.37	Subject and Exoskeleton
Basal Metabolic Rate [W/kg]					*P-value vs. Unsuited*[b]
Unsuited	2.39	1.64	6	0.67	
ExoControl	0.82	0.31	5	0.14	0.067
Exoskeleton	1.23	0.59	6	0.24	0.153
Overall	1.51	0.37	6	0.15	
Partial Gravity Simulation Fidelity					*% Error Relative to Target*
Lunar (Target G=0.165)	0.156	0.03	108	0.003	-5.5
Mars (Target G=0.378)	0.361	0.026	108	0.003	-4.5
Walking Speeds Achieved (Target Fr=0.25)					*% Error Relative to Target*
All	0.281	0.05	54	0.007	12.4
Moon	0.330	0.06	18	0.014	32.0
Mars	0.267	0.01	18	0.002	6.8
Earth	0.246	0.004	18	0.001	-1.6
Running Speeds Achieved (Target Fr = 0.6)					*% Error Relative to Target*
All	0.595	0.101	54	0.014	-0.8
Moon	0.647	0.125	18	0.029	7.8
Mars	0.599	0.038	18	0.009	-0.2
Earth	0.592	0.011	13[c]	0.003	-1.3

[a]Number of parameter values, e.g., number of subjects or number of conditions.

[b]Equality of means t-test assuming unequal variance

[c]After removal of 5 conditions in which subjects did not reach or maintain the assigned speed

Exolocomotion Gait

A more significant limitation of the study was the lack of kinematic (motion tracking) and kinetic (force plate) measurements, which could have been used to estimate center of mass motion and therefore $\dot{W}_{in}$. As a result, estimation of this parameter under non-1g-unsuited conditions required the assumption of dynamic similarity.

Dynamic similarity would strictly require that all non-dimensional parameters associated with gait remain the same. While non-dimensional cadence does not change dramatically with changes in the simulated gravity level, lower g-level was associated with higher Froude numbers at the PTS. This elevation in the Froude number at the PTS for the lunar unsuited condition implies a violation of dynamic similarity at low g-levels.

The observed increase in the median self-selected Froude number with reduced G-level is consistent with the findings of Kram et al. [17], who measured the run-walk transition at a range of simulated gravity levels using a detailed 'titration' procedure to determine the velocity of transition. We used a much more simple procedure due to subject time

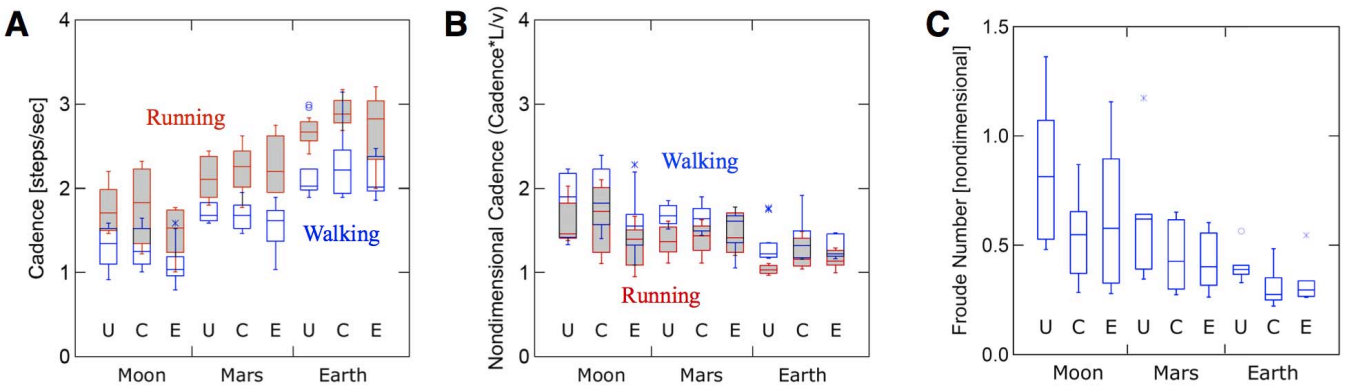

Figure 2. Quartiles for Exoskeleton Gait Parameters as a function of G-level. A) Cadence (steps/s) for walking ($Fr = 0.25$, unfilled boxes) and running ($Fr = 0.60$, filled boxes) conditions. B) Non-dimensional cadence for walking and running as in A. C) Froude Number at the Preferred Transition Speed. In all panels, U = Unsuited, C = ExoControl, E = Exoskeleton. Symbols $*$ and $\circ$ indicate outliers.

Table 2. Specific Resistance Comparison

Condition	$\bar{G}$	$\bar{S}_{actual}$	S_{actual} (Conf. Int.)[a]	S_{theory}	% Difference	p-value[b]
Walking						
Moon	0.140	5.00	$3.64 - 6.37$	5.86	17.2	0.167
Mars	0.348	1.84	$1.12 - 2.57$	1.61	-12.2	0.458
Earth	1.00	0.518	$0.370 - 0.665$	–	–	–
Run/Walk						
Moon	0.168	2.86	$2.13 - 3.59$	2.77	-3.0	0.777
Mars	0.356	1.30	$0.862 - 1.75$	1.21	7.4	0.596
Earth	1.00	0.50	$0.432 - 0.571$	–	–	–
Running						
Moon	0.192	2.78	$2.07 - 3.48$	2.53	-8.7	0.418
Mars	0.367	1.24	$0.917 - 1.56$	1.14	-7.6	0.488
Earth	1	0.46	$0.388 - 0.535$	–	–	–

[a] Confidence interval for the observed values S_{actual}.
[b] One sample equality of means t-test relative to theoretical value ($df = 5$). A p-value < 0.05 would indicate that the mean S value is significantly different than the theoretical value.

Table 3. Mean Unsuited Froude Number at the Preferred Transition Speed

G-Level	This Study	Kram et al.[a]	%Difference
Moon	0.84	0.91	-7.4
Mars	0.62	0.57	8.4
Earth	0.41	0.45	-9.9

[a] Linear interpolation using data from Kram et al. [17].

considerations, and therefore expect less consistent results; the magnitude of the difference between the values observed and the findings of [17] was less than 10% in all gravity conditions (Table 3), and the average difference was only -3%.

Even higher Froude numbers at the PTS were observed in lunar unsuited walking in simulated and actual (parabolic flight) reduced gravity by DeWitt et al. [18]; our lower values, and those of Kram et al. [17] may reflect the approximate nature of our respective partial bodyweight suspension platforms.

Measured cadence values in the $G = 1$ running condition are near optimal for running in Earth gravity [11], supporting the use of $\eta = 0.55$ for running. Walking cadence values are not greatly lower than running cadence values because the $Fr = 0.25$ and $Fr = 0.60$ conditions have a relative velocity ratio of only 0.65. The decline in cadence with reduced G-level is consistent with data reported by [19].

As expected, non-dimensional cadence values for running are slightly less than those for walking. The similarity of non-dimensional cadence values across walking and running, and as a function of the G-level, is an indirect indicator that kinematics may not have changed substantially over the range of conditions studied. The more modest rise in Λ values as gravity is reduced suggests a slight change in the excursion angle, calculated using the Equation 5 approximation as 45-50° for $G = 1$ to 33-40° for $G = 0.165$.

On a whole, there is evidence that dynamic similarity is a reasonable approximation over a range of reduced G-levels but breaks down at low (lunar) G-levels. This can be expected to lead to increasing errors in $\dot{W}_{in}$ at low G-levels, and errors in $\dot{W}_{in}$ would be expected to lead to commensurate errors in recovery, η (see Equation 13). In practice it would be better to measure $\dot{W}_{in}$ directly.

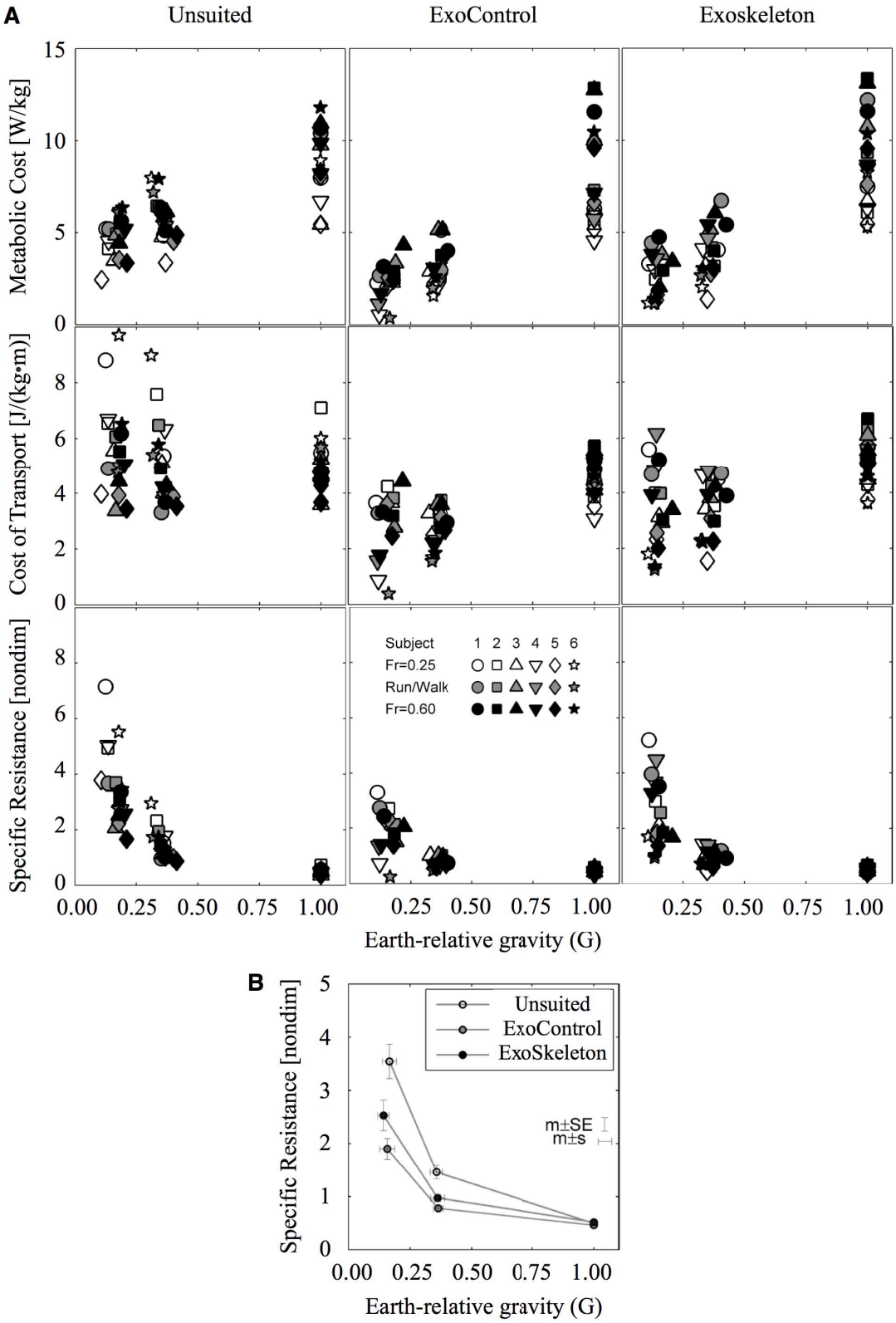

Figure 3. Energetics of Exoskeleton Locomotion. A) Top row: Mass-specific metabolic cost $[W/kg]$. Center row: Cost of transport $[J/(kg \cdot m)]$. Bottom row: Specific resistance. In all panels, unfilled symbols represent the walking ($Fr = 0.25$) condition, gray-filled symbols represent the run-walk condition ($Fr = 0.50$), and black-filled symbols represent the running ($Fr = 0.60$) condition. B) Specific resistance values, averaged across all subjects and all Froude number conditions within each combination of exoskeleton configuration and G-level, reveal the significant cross-effect between the exoskeleton conditions and the G level.

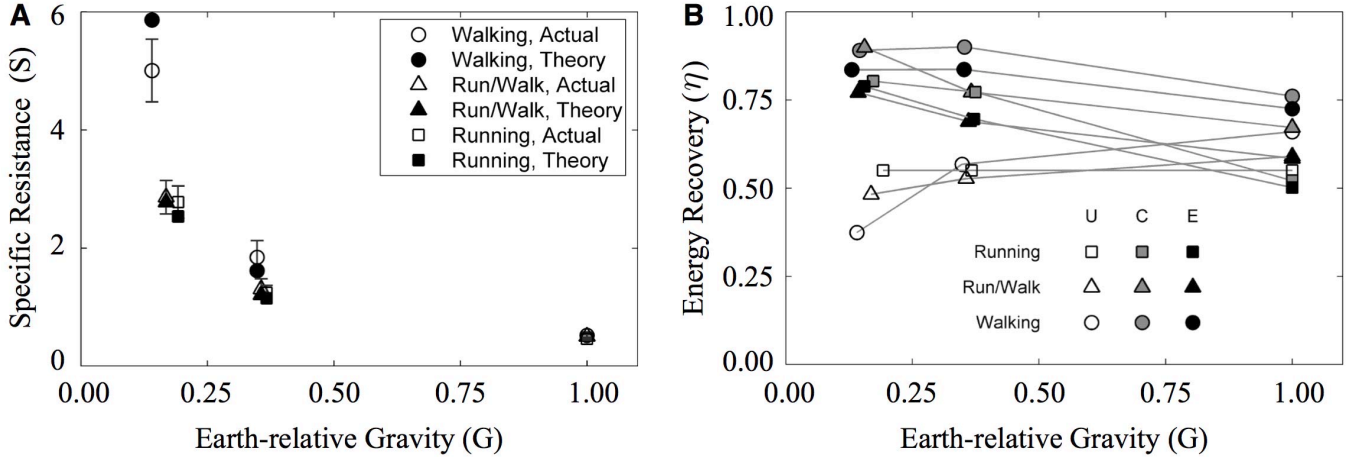

Figure 4. Model and Energy Recovery Comparison. A) Unsuited specific resistance as a function of G-level: Unfilled symbols represent values computed directly from metabolic data. Filled symbols, the theoretical values, were estimated based on the $G = 1$ data using the approach described in the methods. Thus, theoretical results are shown only for the reduced gravity conditions. Error bars, one per actual measurement, are $m \pm SE$. B) Computed net energy recovery ratio as a function of G-level and exoskeleton condition: Exoskeleton conditions are denoted by U (Unsuited, unfilled symbols), C (ExoControl, grey symbols), and E (Exoskeleton, black symbols).

Exolocomotion Energetics

One surprising feature of the energetics results was that cost of transport at constant Froude numbers was relatively independent of G-level in the unsuited condition. This is different, but does not contradict, the relatively linear declines observed in the *constant velocity* reduced gravity walking and running measurements by Farley and McMahon [16].

The success of the theoretical predictions of specific resistance values across all Froude number conditions, without any statistical differences between the observed and predicted values, suggests that the mathematical form of the model is reasonable, and that reasonable parameter values have been chosen. The goodness of fit (Adjusted R^2 of 0.98 for measured versus theoretical S) is somewhat surprising, because of the nature and extent of the assumptions that went into the estimates: First, they assume a very crude derivation of the gravitational dependence of muscle efficiency (see Appendix B). Second, the model as implemented to date is based on an assumption of 55% energy recovery during running, with no compensation for G or velocity; the data on walking energy recovery from [10] is much more extensive. Third, when the total positive work rate by locomotion muscles ($\dot{W}_{in}$) was transformed from one state to another, $\dot{W}_{in}$ was assumed to scale directly with the gravity and mass ratios of the two conditions, making an implicit assumption of dynamic similarity, which is clearly an approximation. Nevertheless, a single equation,

$$\dot{Q}_m - \dot{Q}_b = \dot{W}_{in} \cdot \frac{1-\eta}{E_{musc}}$$

successfully predicted the observed metabolic cost across G and v, and across both walking and running gaits.

Perhaps the most surprising energetics results was the large impact of the low-stiffness springs used in the ExoControl condition. It was not anticipated that they would affect cost of transport and other variables to the extent that they did. The ExoControl springs were not calibrated to measure EMU-relative stiffness, but by basic beam theory should be approximately 2^{-3} as stiff as the Exoskeleton springs, which on average approximate the EMU knee joints and have peak stiffness values of 1-5 kN/m, depending on the leg geometry. The ExoControl exoskeleton legs appear to have very high energy recovery, and several subjects commented on their relative easy of movement in reduced gravity; one subject described wearing these legs while walking in reduced gravity as 'effortless...I forgot they were there.'

It is possible that net energy recovery ratios are overestimated due to increases in $\dot{W}_{in}$ relative to the similar unsuited condition. However, [10] found that vertical displacements of the center of mass changed by less than 10% during simulated reduced gravity walking in the range $0.25 \leq G \leq 1.0$. While the observed net energy recovery ratios are high, they are consistent with the measured recovery values for the exoskeleton legs [7]. An open question is whether each exoskeleton leg can store enough energy to account for a significant fraction of $\dot{W}_{in}$ during reduced gravity locomotion; this value has not been computed, but could be estimated if reliable kinematics data were available. It is possible that the ExoControl exoskelton legs have appropriate stiffness to simultaneously improve recovery and permit normal kinematics.

Why does the unsuited run-walk transition occurs at higher Froude numbers at low (Lunar) gravity? Or equivalently, why does dynamic similarity fail? One explanation is that at low gravity, for similar $\dot{W}_{in}$, the normal exchange of kinetic and potential energy during pendular walking is impaired. Another component is inertial forces: The swinging of arms and legs creates a downward force that helps keep the body on the ground during reduced gravity walking, and this effect is magnified in a center-of-mass partial-body-weight suspension system in which the arms and legs are acted upon by normal levels of gravity. Kram et al. [17] estimated the size of this effect for humans locomoting in reduced gravity, and used it to compute corrected run-walk transition Froude numbers, which were nearly constant (≈ 0.5) over a ten-fold range of gravity.

How do these findings relate to space suit energetics? All the same mechanisms at work in exoskeleton locomotion apply to (soft-goods) space suit legs. For example, space suit legs have high energy recovery and similar knee joint stiffness. In addition, extensive analysis of gait events during Project Apollo reveals that the walk or lope to run transition by space-suited astronauts on the Lunar surface is estimated to be $Fr = 0.36 \pm 0.11$ [20]. Just as the exoskeleton lowered the PTS (Figure 2C), space suits lower the PTS.

Major differences between the exoskeleton and space suits include the much higher mass, impaired hip, ankle, and upper body mobility, and the presence of longitudinal pressure forces; these and other differences between space suits and the lower-body exoskeleton are reviewed and summarized in [7]. Space suits are likely to improve recovery during locomotion, but to do so in an unbalanced way with respect to walking and running: while running energy recovery may be enhanced, the impaired hip and ankle mobility may greatly impair energy recovery during walking [5], [6], making a transition to running favorable at lower Fr than under unsuited conditions.

The Tuned Space Suit

The current study has an important implication for future space suit design: it provides a new start to answering the question: What is the optimal space suit joint torque? One of the mantras of space suit design for more than the last forty years has been to 'eliminate joint-torques,' based on the assumption that the best joint-torque is no joint torque. However, as Figure 5 illustrates, this is not necessarily the case when one considers lowering the metabolic cost of locomotion as an objective.

Consider an ideal space suit with lower legs whose stiffness can be adjusted from zero to beyond the value achieved in the Exoskeleton condition. With zero 'suit' (or exoskeleton) leg stiffness, the unsuited specific resistance is achieved. As the stiffness increases, some energy is stored in and released by the high-recovery exoskeleton or suit leg, slightly improving overall recovery and lowering S. Stiffness must decline because the observed S in the ExoControl condition is lower than the unsuited S. At some stiffness level, a minimum is achieved, but the available constraints make it impossible to determine whether the optimal stiffness is smaller or larger in magnitude than the effective stiffness of the ExoControl exoskeleton legs. For this reason, two representative gray curves are shown in Figure 5. It is likely the optimal stiffness is greater than the ExoControl exoskeleton leg stiffness (solid gray curve), based on subjective feel and the ~8-fold difference in stiffness between the ExoControl condition and the Exoskeleton condition. As stiffness increases further, S must increase because under the Exoskeleton condition the exoskeleton legs are approximately eight times more stiff than under the ExoControl condition, and the observed S under the Exoskeleton condition is larger than the ExoControl condition. As the stiffness increases further, the greater stiffness of the suit or exoskeleton legs will disrupt normal kinematics more and more, until recovery and/or biomechanical advantage is impaired, resulting in a higher specific resistance. The extent to which the ideal stiffness would change with the G-level is unknown.

How would one go about creating a Tuned Space Suit? Modifying the thickness of the exoskeleton fiberglass bars and making additional measurements of specific resistance is one possibility. Another is to address the general problem of how springs in parallel with the legs change leg stiffness (Figure 5B), k_{leg}, what changes this implies to regulation of effective total leg stiffness, $k_{eff} = k_{leg} + k_{suit}$, and how these changes might effect the metabolic cost of locomotion.

Human leg stiffness, based on a mass-spring model of running [21], [22], changes little with velocity [22], but does accommodate changes in surface stiffness [23], [24]. Ferris and Farley [23] found that humans maintained similar vertical center of mass displacement despite a > 1000 fold change in surface stiffness k_{surf}.

What happens if regulation of k_{leg} is intentionally disrupted? McMahon et al. [15] had subjects run with their knees bent ('Groucho' style, something they wouldn't normally do on their own), thereby reducing their leg stiffness to 82% of normal. This incurred a oxygen consumption penalty of up to 50% above 'normal' running, presumably because the lower leg stiffness led to larger oscillations of the center of mass ($\dot{W}_{in}$ increased, resulting in a higher $\dot{Q}_m - \dot{Q}_b$ for the same E_{musc} and η).

Like Ferris and Farley [23], Kerdok et al. [25] found that effective leg stiffness, k_{eff}, was the same despite variations in the surface stiffness. As surface stiffness decreased, leg stiffness increased, resulting in a similar effective leg stiffness ($1/k_{eff} = 1/k_{leg} + 1/k_{surf}$, because the leg and surface are in series, e.g., Figure 5C). Over the range of k_{surf} tested (75.4-946 kN/m) Kerdok et al. [25] found a drop in metabolic rate of 12% as k_{surf} was decreased.

Constant k_{eff} in the McMahon and Cheng [22] running model implies similar magnitude oscillations of the center of mass (similar W_{in} per step), suggesting that the metabolic cost reduction found by Kerdok et al. [25] results from increased recovery (η); Kerdok et al. [25] computed energy delivery by the compliant surface, and found that for every watt delivered by the surface, the metabolic rate decreased by 1.8W. This same calculation could be performed for exoskeleton legs using data from trials for which kinematic data are available.

It is not known how humans modify leg stiffness in response to springs in parallel with the legs; however, to maintain the same center of mass motion, one would expect the response to be a reduction in k_{leg} that results in the 'normal' k_{eff} at the current G level. Donelan and Kram [26] reported leg stiffness values for 2-5 m/s running: Earth-gravity stiffness values of 8-10 kN/m had declined to approximately 5.0-6.5 kN/m in $G = 0.25$. Because the EMU-like exoskeleton springs have stiffnesses in the range of several kN/m, they could be expected to have a significant effect on k_{leg}. Studying changes in k_{leg} in response to springs in parallel with the legs might lead to a better understanding of human leg stiffness regulation, in addition to determining whether it is feasible or desirable to build a tuned space suit.

McMahon et al. [15] and Kerdok et al. [25] have connected regulation of leg stiffness to the metabolic cost of locomotion, but the definitive theoretical and experimental link between leg stiffness, recovery, and metabolic cost has yet to be made. While such a link is beyond the scope of this work, further discussion about recovery and its impact beyond the exoskeleton experiment is in order.

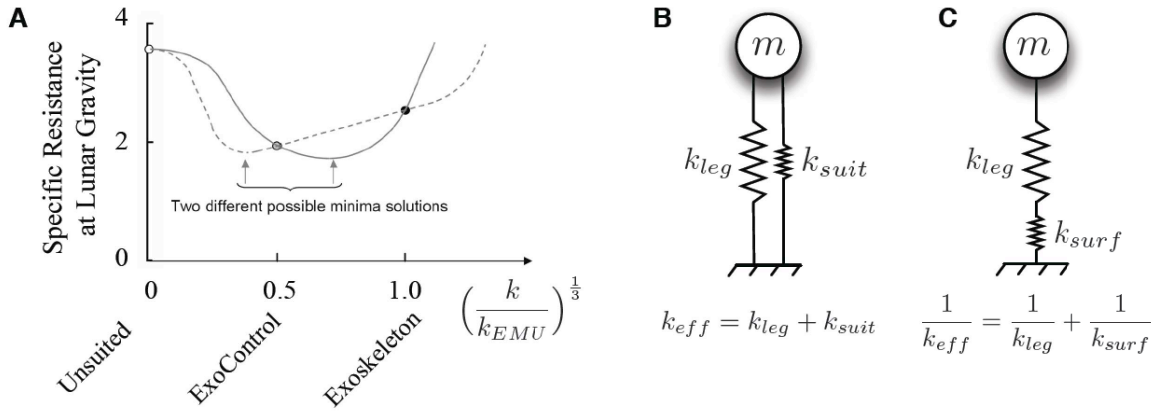

Figure 5. **The Tuned Space Suit. A) The mean specific resistance values (averaged across Fr and subject) observed in the Lunar ($G = 0.165$) condition show a non-linear relationship with EMU relative stiffness k/k_{EMU}. Unsuited specific resistance was observed to be higher than both exoskeleton configurations, with the ExoControl specific resistance lower than the Exoskeleton specific resistance. This implies that an exoskeleton leg stiffness exists, below the leg stiffness of the Exoskeleton configuration, which has minimum specific resistance. A similar finding may apply to space suits; at this point such as 'Tuned Space Suit' would be energetically optimal. B) Spring-mass model of human interaction with an exoskeleton or space-suit. C) Spring-mass model of human interaction with a compliant surface.**

5. CONCLUSIONS

Here we have presented a simple model of locomotion energetics, for which our predictions based on dynamic similarity match measured energetics across gravity and gait, with errors higher at low gravity where dynamic similarity is violated. While dynamic similarity is a useful assumption to enable estimation of certain parameters in our model, future work will benefit from direct kinematic and kinetic measurements.

We then used this model to characterize how a lower-body exoskeleton modifies the energetics of walking and running, in particular through changing the energy recovery, a measure of the reversibility of work done on the center of mass during locomotion. In keeping with our hypothesis, we found that springs in parallel with human legs, as represented by a lower body exoskeleton, can improve energy recovery and decrease the metabolic cost of transport. This led to the notion of a tuned space suit, where the exoskeleton or space suit stiffness could be adjusted to achieve a local minima in the cost of transport.

We note that while gas pressure space suit legs inherently function like springs, mechanical counter-pressure space suits, which apply pressure directly to the body surface, could be augmented with an external exoskeleton. Thus, our findings apply to both types of space suits. Lower body hard suits, in contrast, are likely to have effective spring stiffness beyond the optimal range for human locomotion. Energy efficient locomotion is a key requirement for future planetary exploration; ultimately, many factors will need to be considered in the design and development of space suits for future human planetary exploration.

APPENDICES

A. HILL MUSCLE MODEL

In the same year in which he received the Nobel Prize "for his discovery relating to the production of heat in the muscle"[2], A.V. Hill demonstrated that muscles are most efficient for a particular range of the muscle velocity of shortening, v [27]. Hill later related the tension (force) produced by muscle undergoing an isotonic contraction, T, to the velocity of shortening [28] as:

$$(T + a) \cdot (T + b) = (T_0 + a) \cdot b, \tag{14}$$

where T_0 is isometric muscle tension, and a and b are constants. Geometrically, this equation represents a rectangular hyperbola with asymptotes of $T = -a$ and $T = -b$ [29]. With no load ($T = 0$) the maximum shortening velocity v_{max} is achieved. Rewriting Equation 14 in terms of normalized velocity v/v_{max} and normalized tension T/T_0 gives:

$$\frac{v}{v_{max}} = \frac{1 - T/T_0}{1 + (T/T_0) \cdot k^{-1}}, \tag{15}$$

where $k = a/T_0 = b/v_{max}$. Equations 14 and 15 apply to nearly all types of muscles in non-insects, including skeletal, cardiac, and smooth muscle [29].

The load-dependence of the myosin stroke relative to its actin fiber is the primary molecular determinant of the mechanical performance and efficiency of skeletal muscle [30]. This provides a molecular basis for the observation that $0.15 < k \leq 0.25$ for most vertebrate muscles [29], although Alexander [31] recommends $k = 0.25$ as a good average value for vertebrate muscles.

Because muscles share a common architecture within and across organisms and species, but differ in the types and proportions of protein isoforms upon which the common architecture depends, it seems reasonable that Equations 14 and 15 are so widely applicable. Leeuwen and Spoor [32] expressed Equation 15 in a different form and developed a related expression that takes into account the possibility of negative shortening velocities (muscle lengthening, or eccentric motion):

[2] **See http://www.nobel.se/medicine/laureates/1922/**

$$\frac{T}{T_0} = \begin{cases} \frac{v_{max}-v}{v_{max}+Gv} & 0 \le v \le v_{max} \\ 1.8 - 0.8 \cdot \left[\frac{v_{max}+v}{v_{max}-rGv}\right] & -v_{max} < v < 0 \end{cases} \tag{16}$$

where $G = 1/k$, and $r = 7.56$ is a factor that reflects the mechanics of eccentric motion.

For an isotonic (constant tension) contraction of a muscle in which all muscle fibers are oriented uniformly, so that the velocity of shortening and the tension are collinear, mechanical power output, $\dot{W}$, can be computed as

$$\begin{aligned} \dot{W} &= \frac{d}{dt}\int \vec{T}\cdot\vec{dl} \\ &= T\frac{d}{dt}\int dl \\ &= T\frac{dl}{dt} \\ &= Tv \end{aligned} \tag{17}$$

where l is muscle length and t is time. In order to evaluate how the efficiency of muscle is linked to the parameters of the Hill equation (Equation 14), Alexander [33] defined muscle efficiency as the ratio of mechanical power to metabolic power consumption of a fully activated muscle, P_{metab}, assuming adenosine tri-phosphate (ATP) as the energy source. The efficiency of production of ATP from aerobic respiration and foodstuffs, η_{ATP}, is only about 50% efficient [31], so that the net efficiency from the rate of enthalpy change to muscular work is given by

$$E_{musc} = \eta_{ATP}\frac{\dot{W}}{P_{metab}}. \tag{18}$$

Alexander [33] expressed P_{metab} as:

$$P_{metab} = T_0 v_{max}\Phi(v/v_{max}), \tag{19}$$

and then derived empirical expressions for Φ based on the data of Ma and Zahalak [34]:

$$\Phi(\frac{v}{v_{max}}) = \begin{cases} 0.23 - 0.16\cdot e^{\left(-8\cdot\frac{v}{v_{max}}\right)} \\ 0.01 - 0.11\cdot\frac{v}{v_{max}} \\ +0.06\cdot e^{\left(23\cdot\frac{v}{v_{max}}\right)} \end{cases} \tag{20}$$

where, as in Equation 16, the top expression applies for $0 \le v \le v_{max}$ and the bottom expression applies for $-v_{max} < v < 0$. Using Equations 17 and 19, Equation 18 can be rewritten as

$$E_{musc} = \eta_{ATP}\cdot\frac{T}{T_0}\cdot\frac{v}{v_{max}}\cdot\frac{1}{\Phi(v/v_{max})}. \tag{21}$$

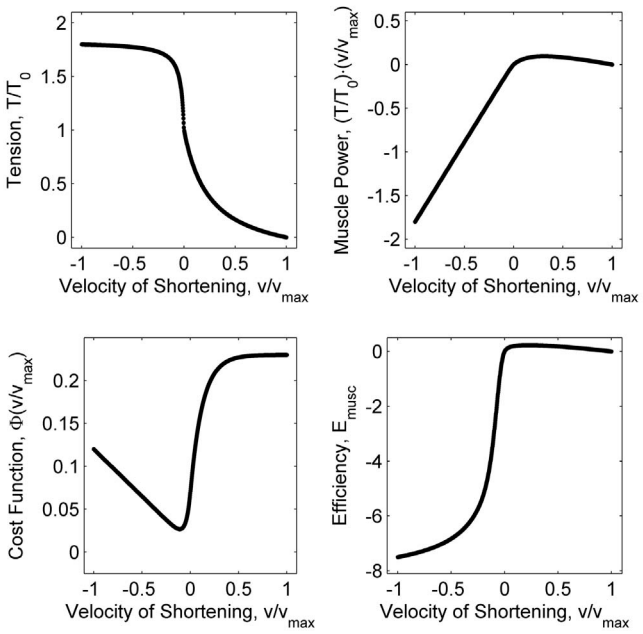

Figure 6. Parameters of the Hill muscle model as a function of v/v_{max}, the ratio of muscle contraction velocity to maximum muscle contraction velocity. T/T_0 is the ratio of muscle tension to isometric tension, Φ is a cost function describing cellular energetics, and E_{musc} is the muscle efficiency.

Using $G = 4$ ($k = 0.25$) and $r = 7.56$ gives maximum $E_{musc} = 0.225$ for $v/v_{max} = 0.227$ and maximum normalized power $\dot{W}/(T_0 v_{max}) = 0.096$ for $v/v_{max} = 0.311$. The hill muscle model as computed using these parameters is shown in Figure 6. The peak efficiency and peak power values are best visualized in a plot restricted to positive contraction velocities, as illustrated in Figure 7.

B. Muscle Efficiency & Gravity

Here we describe a derivation for the dependence of muscle efficiency E_{musc} on gravity.

We assume that muscles operate at near peak efficiency under $G = 1$ conditions. This is a reasonable assumption, as illustrated by the agreement, to within 2-3%, between the maximum muscular efficiency observed during slope walking [12] or cycling [13] and the peak efficiency predicted by the above-implemented Hill Muscle Model.

In addition, this model assumes that no substantial shifts in muscle mass or remodeling (change in fiber type) have occurred. This is a reasonable assumption for our experiment, where subjects only briefly encountered simulated reduced gravity, but would not hold during spaceflight or on Mars, where long exposure to weightlessness or reduced gravity would produce shifts in the types of muscle fibers present and in total muscle mass. Indeed, reductions in muscle mass seen in spaceflight can be seen as an adaptive response to achieve more efficient muscle activation.

To simulate the effects of reduced gravity on muscle, the T/T_0 value at the $G = 1$ peak efficiency condition can be

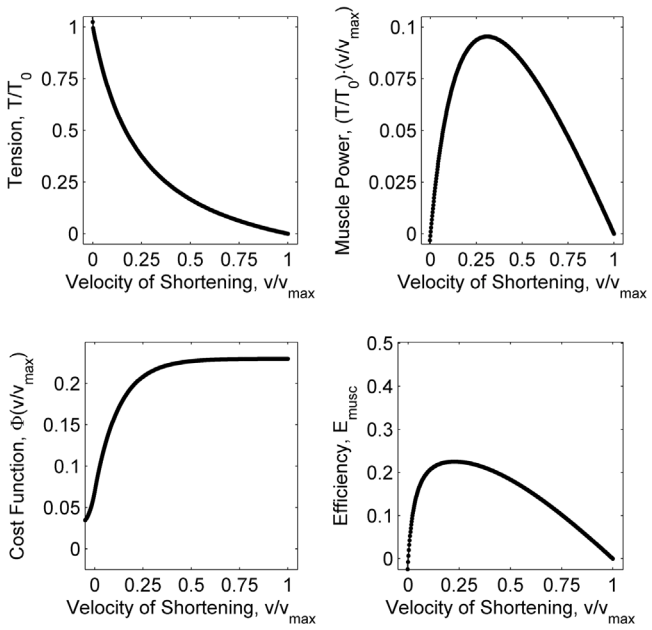

Figure 7. Hill muscle model for positive muscle contraction velocities. v/v_{max} is the ratio of muscle contraction velocity to maximum muscle contraction velocity, T/T_0 is the ratio of muscle tension to isometric tension, Φ is a cost function describing cellular energetics, and E_{musc} is the muscle efficiency. Peak efficiency is 0.23 for $v/v_{max} = 0.23$. Peak power occurs at $v/v_{max} = 0.31$ and $E_{musc} = 0.22$.

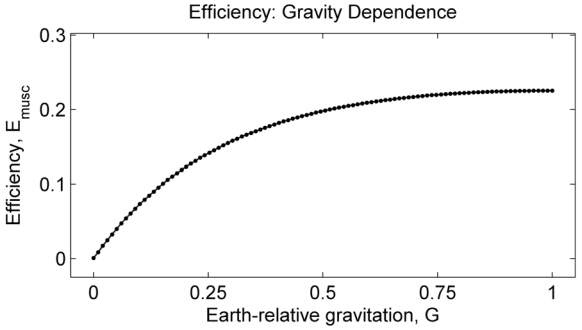

Figure 8. Gravitational dependency of muscle efficiency derived from the Hill Model.

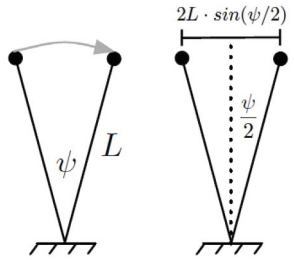

Figure 9. Excursion angle in idealized compass gait. In inverted pendulum walking, with no double support and no aerial phase, a leg with length L traces out an excursion angle ψ during a single stance period.

scaled so that the new 'reduced gravity' tension ratio is

$$\frac{T\prime}{T_0} = G \cdot \left(\frac{T}{T_0}\right)_{1G, E_{Peak}}. \tag{22}$$

From $T\prime/T_0$ a new v/v_{max} can be estimated using Equation 15, allowing E_{musc} to be computed as a function of G (Figure 8).

Why might the muscle efficiency vary with G but not vary substantially with locomotion velocity?[3] McMahon and others have shown that leg stiffness, but not vertical stiffness [22] is relatively constant as a function of velocity. Leg stiffness is related to contraction velocity, and therefore muscle efficiency can be maintained across a wide range of velocities.

C. Non-Dimensional Cadence

Here we describe a derivation for the non-dimensional cadence $\Lambda = fL/v$ (Eq. 4), with step frequency f, subject leg length L, and gait velocity v. In idealized compass gait (Figure 9), ψ is the excursion angle swept out by the leg during a single stance period. The horizontal movement of the center of mass, equivalent to the distance per step, is given by $v/f = 2L \cdot sin(\psi/2)$, and thus the non-dimensional cadence is given by $\Lambda = 1/(2 \cdot sin(\psi/2))$ (Eq. 4).

[3]Assuming that velocity is not too small.

Acknowledgments

The authors thank the anonymous reviewers for their helpful comments.

References

[1] "NASA's Journey to Mars," Washington, DC, Tech. Rep. NP-2015-08-2018-HQ, 2015.

[2] E. Musk, "Making Humans a Multiplanetary Species." 67th IAC, Guadalajara, Mexico, Sep. 2016.

[3] C. E. Carr, A. Mojarro, J. Tani, S. A. Bhattaru, M. T. Zuber, R. Doebler, M. Brown, K. Herrington, R. Talbot, C. W. Fuller, M. Finney, G. Church, and G. Ruvkun, "Advancing the Search for Extra-Terrestrial Genomes," in *IEEE Aerospace Conference*, Big Sky, Montana, 2016, pp. 1–15.

[4] A. Mojarro, G. Ruvkun, M. Zuber, and C. Carr, "Human Exploration of Mars at Valles Marineris: The Past, Present, and Future of Life on Mars," in *First Landing Site/Exploration Zone Workshop for Human Missions to the Surface of Mars*, Houston, TX, Oct. 2015, pp. Oct 27–30.

[5] C. E. Carr and D. J. Newman, "Space suit bioenergetics: framework and analysis of unsuited and suited activity," *Aviation, Space, and Environmental Medicine*, vol. 78, no. 11, pp. 1013–1022, Nov. 2007.

[6] ——, "Space suit bioenergetics: cost of transport during walking and running," *Aviation, Space, and Environmental Medicine*, vol. 78, no. 12, pp. 1093–1102, Dec. 2007.

[7] C. Carr and D. Newman, "Characterization of a lower-

body exoskeleton for simulation of space-suited locomotion," *Acta Astronautica*, vol. 62, pp. 308–323, 2008.

[8] P. Schmidt, "An Investigation of Space Suit Mobility with Applications to EVA Operations," Doctoral Dissertation, Massachusetts Institute of Technology, 2001.

[9] C. E. Carr, "The bioenergetics of walking and running in space suits," Ph.D. dissertation, Massachusetts Institute of Technology, Cambridge, MA, 2005, http://dspace.mit.edu/handle/1721.1/33088.

[10] T. M. Griffin, N. A. Tolani, and R. Kram, "Walking in simulated reduced gravity: mechanical energy fluctuations and exchange," *J Appl Physiol*, vol. 86, no. 1, pp. 383–90, 1999.

[11] M. Kaneko, "Mechanics and energetics in running with special reference to efficiency," *J Biomech*, vol. 23 Suppl 1, pp. 57–63, 1990.

[12] R. Margaria, *Biomechanics and Energetics of Muscular Exercise*. Oxford, England: Clarendon Press, 1976.

[13] F. Whitt and D. Wilson, *Bicycling Science*. Cambridge, Massachusetts: The MIT Press, 1982.

[14] R. Wu, "Human Readaptation to Normal Gravity Following Short-Term Simulated Martian Gravity Exposure and the Effectiveness of Countermeasures," S.M. Thesis, Massachusetts Institute of Technology, 1999.

[15] T. A. McMahon, G. Valiant, and E. C. Frederick, "Groucho running," *J Appl Physiol*, vol. 62, no. 6, pp. 2326–37, 1987.

[16] C. T. Farley and T. A. McMahon, "Energetics of walking and running: insights from simulated reduced-gravity experiments," *J Appl Physiol*, vol. 73, no. 6, pp. 2709–12, 1992.

[17] R. Kram, A. Domingo, and D. P. Ferris, "Effect of reduced gravity on the preferred walk-run transition speed," *J Exp Biol*, vol. 200, no. Pt 4, pp. 821–6, 1997.

[18] J. K. De Witt, W. B. Edwards, M. M. Scott-Pandorf, J. R. Norcross, and M. L. Gernhardt, "The preferred walk to run transition speed in actual lunar gravity." *J Exp Biol*, vol. 217, no. Pt 18, pp. 3200–3203, Sep. 2014.

[19] B. L. Davis and P. R. Cavanagh, "Simulating reduced gravity: a review of biomechanical issues pertaining to human locomotion," *Aviat Space Environ Med*, vol. 64, no. 6, pp. 557–66, 1993.

[20] C. Carr and J. McGee, "The Apollo Number: Space Suits, Self-Support, and the Walk-Run Transition," *PLoS ONE*, vol. 4, no. 8, pp. e6614 EP–, Aug. 2009.

[21] R. Blickhan, "The spring-mass model for running and hopping," *J Biomech*, vol. 22, no. 11-12, pp. 1217–27, 1989.

[22] T. A. McMahon and G. C. Cheng, "The mechanics of running: how does stiffness couple with speed?" *J Biomech*, vol. 23 Suppl 1, pp. 65–78, 1990.

[23] D. P. Ferris and C. T. Farley, "Interaction of leg stiffness and surfaces stiffness during human hopping," *J Appl Physiol*, vol. 82, no. 1, pp. 15–22; discussion 13–4, 1997.

[24] C. T. Farley, H. H. Houdijk, C. Van Strien, and M. Louie, "Mechanism of leg stiffness adjustment for hopping on surfaces of different stiffnesses," *J Appl Physiol*, vol. 85, no. 3, pp. 1044–55, 1998.

[25] A. E. Kerdok, A. A. Biewener, T. A. McMahon, P. G. Weyand, and H. M. Herr, "Energetics and mechanics of human running on surfaces of different stiffnesses," *J Appl Physiol*, vol. 92, no. 2, pp. 469–78, 2002.

[26] J. M. Donelan and R. Kram, "Exploring dynamic similarity in human running using simulated reduced gravity," *J Exp Biol*, vol. 203, no. Pt 16, pp. 2405–15, 2000.

[27] A. Hill, "The maximum work and mechanical efficiency of human muscles, and their most economical speed." *J Physiology*, vol. 56, pp. 19–41, 1922.

[28] ——, "The heat of shortening and the dynamic constants of muscle," *Proceedings of the Royal Society of London*, vol. B126, pp. 136–195, 1938.

[29] T. McMahon, *Muscles, Reflexes, and Locomotion*. Princeton, New Jersey: Princeton University Press, 1984.

[30] M. Reconditi, M. Linari, L. Lucii, A. Stewart, Y. B. Sun, P. Boesecke, T. Narayanan, R. F. Fischetti, T. Irving, G. Piazzesi, M. Irving, and V. Lombardi, "The myosin motor in muscle generates a smaller and slower working stroke at higher load," *Nature*, vol. 428, no. 6982, pp. 578–81, 2004.

[31] R. Alexander, *Principles of Animal Locomotion*. Princeton, New Jersey: Princeton University Press, 2003.

[32] J. L. Van Leeuwen and C. W. Spoor, "Modelling mechanically stable muscle architectures," *Philos Trans R Soc Lond B Biol Sci*, vol. 336, no. 1277, pp. 275–92, 1992.

[33] R. Alexander, "Optimum muscle design for oscillatory movements," *J Theor Biol*, vol. 184, no. 3, pp. 253–259, 1997.

[34] S. P. Ma and G. I. Zahalak, "A distribution-moment model of energetics in skeletal muscle," *J Biomech*, vol. 24, no. 1, pp. 21–35, 1991.

BIOGRAPHY

Christopher E. Carr *received the B.S. degree in Aero/Astro and the B.S. degree in Electrical Engineering in 1999, the M.S. degree in Aero/Astro in 2001, and the Sc.D. degree in Medical Physics in 2005, all from MIT. He is a Research Scientist at MIT in the Department of Earth, Atmospheric and Planetary Sciences and a Research Fellow at the Massachusetts General Hospital in the Department of Molecular Biology. He is broadly interested in searching for and expanding the presence of life beyond Earth.*

Dava J. Newman *received a B.S. in Aerospace Engineering from U. Notre Dame in 1986, the S.M. in Aeronautics & Astronautics, and the S.M. in Technology and Policy, from MIT in 1989, and the Ph.D. in Aerospace Biomedical Engineering from MIT in 1992. She has served as the Deputy Administrator of the National Aeronautics and Space Administration since April, 2015. Prior to that time, she was the Apollo Program Professor of Astronautics at MIT.*